Published in final edited form as:
Nature. 2012 September 27; 489(7417): 526–532. doi:10.1038/nature11414.

Neutralization of influenza A viruses by insertion of a single antibody loop into the receptor binding site

Damian C. Ekiert[1,*,+], **Arun K. Kashyap**[2,*], **John Steel**[3,‡], **Adam Rubrum**[4], **Gira Bhabha**[1], **Reza Khayat**[1], **Jeong Hyun Lee**[1], **Michael A. Dillon**[2,§], **Ryann E. O'Neil**[2,¶], **Aleksandr M. Faynboym**[2], **Michael Horowitz**[2], **Lawrence Horowitz**[2], **Andrew B. Ward**[1], **Peter Palese**[3], **Richard Webby**[4], **Richard A. Lerner**[5,6], **Ramesh R. Bhatt**[2], and **Ian A. Wilson**[1,6]

[1]Department of Molecular Biology, The Scripps Research Institute, 10550 North Torrey Pines Road, La Jolla, CA 92037, USA

[2]Sea Lane Biotechnologies, 2450 Bayshore Parkway, Mountain View, CA 94043, USA

[3]Department of Microbiology, Mount Sinai School of Medicine, 1 Gustave Levy Place, New York, NY 10029–6574

[4]Department of Infectious Diseases, St. Jude Children's Research Hospital, 262 Danny Thomas Place, Memphis, TN 38105 USA

[5]Department of Chemistry, The Scripps Research Institute, 10550 North Torrey Pines Road, La Jolla, CA 92037, USA

[6]The Skaggs Institute for Chemical Biology, The Scripps Research Institute, 10550 North Torrey Pines Road, La Jolla, CA 92037, USA

Summary

Immune recognition of protein antigens relies upon the combined interaction of multiple antibody loops, which provides a fairly large footprint and constrains the size and shape of protein surfaces that can be targeted. Single protein loops can mediate extremely high affinity binding, but it is unclear whether such a mechanism is available to antibodies. Here we report the isolation and

Correspondence and requests for materials should be addressed to I.A.W. (wilson@scripps.edu) or R.R.B. (ramesh.bhatt@sealanebio.com).
*These authors contributed equally to this work.
+Present address: Department of Microbiology and Immunology, University of California-San Francisco, 600 16th St., San Francisco, CA 94143
§Present address: Genentech Inc., 1 DNA Way, South San Francisco, CA 94080
¶Present address: Novartis Institutes for BioMedical Research, 4560 Horton Street, Emeryville, CA 94608
‡Present address: Department of Microbiology and Immunology, Emory University School of Medicine, 3103 Rollins Research Center, 1510 Clifton Road, 194-001- 1AD, Atlanta, GA 30322

Author Contributions: A.K.K., M.A.D., R.E.O., A.M.F., M.H., L.H., R.A.L., and R.R.B. isolated and performed the initial characterization of C05; A.K.K., J.S., A.R., P.P., and R.W. designed and performed virus neutralization and *in vivo* experiments; D.C.E. M.A.D., R.E.O., A.M.F and A.K.K. expressed and purified proteins; D.C.E. determined and analyzed the crystal structures with guidance of I.A.W.; G.B., D.C.E., M.A.D., R.E.O., A.M.F and A.K.K. performed binding experiments; R.K., J.H.L. and A.B.W. carried out EM studies; D.C.E. and A.K.K. analyzed the sequence datasets; D.C.E., I.A.W, R.R.B, and A.K.K. wrote the manuscript. All authors commented on the paper.

Author Information: Coordinates and structure factors have been deposited in the Protein Data Bank (PDB codes 4FNK, 4FNL, 4FP8, and 4FQR). EM maps have been deposited in the EMDB (accession nos. 2138, 2139, and 2140). Nucleotide sequences for the C05 variable regions have been deposited in GenBank (accession nos. JX206996 and JX206997). Reprints and permissions information is available at www.nature.com/reprints. The authors declare competing financial interests: A.K. Kashyap, M.A. Dillon, R.E. O'Neil, A.M. Faynboym, M. Horowitz, L. Horowitz, and R.R Bhatt are employees or former employees of Sea Lane Biotechnologies. Readers are welcome to comment on the online version of this article at www.nature.com/nature.

Supplementary Information is linked to the online version of the paper at www.nature.com/nature.

characterization of antibody C05 that neutralizes strains from multiple subtypes of influenza A viruses, including H1, H2, and H3. Crystal and EM structures show that C5 recognizes conserved elements of the receptor binding site on the hemagglutinin (HA) surface glycoprotein. Recognition of the HA receptor binding site is dominated by a single HCDR3 loop, with minor contacts from HCDR1, and is sufficient to achieve nanomolar binding with a minimal footprint. Thus, binding predominantly with a single loop can allow antibodies to target small, conserved, functional sites on otherwise hypervariable antigens.

Introduction

Antibody recognition of protein antigens is predominantly mediated by four to six complementarity determining regions (CDRs), which are the variable loops at the tip of each antigen binding fragment (Fab). The relatively large footprint of antibodies on their target antigens (~700–900 Å^2 for proteins) generally correlates with high affinity binding. However, for neutralizing antibodies against variable pathogens, a larger footprint may result in increased opportunity for escape mutations that reduce antibody binding. Moreover, functionally conserved sites on otherwise variable antigens may be small, as for the influenza virus receptor binding site, partially protected by glycans as in HIV-1 gp 120 and influenza, or are sterically restricted and difficult for antibodies to access, such as the picornavirus "canyon"[1] or the gp 120 co-receptor binding site on HIV-1[2]. In contrast, non-immunoglobulin proteins can also achieve high affinity binding in other ways that may have distinct advantages for targeting small, constrained surfaces. For example, bovine pancreatic trypsin inhibitor (BPTI) attains exceptionally high affinity binding (femtomolar) to serine proteases by inserting a single loop into the enzyme active site[3]. In light of the increasingly long, heavy chain CDR3 (HCDR3) loops being found in humans[4–6], a BPTI-like binding mechanism may be structurally accessible to antibodies, allowing insertion of a single loop into a pocket. However, no clear example of an antibody using such a binding mechanism has been reported.

Two conserved and functionally important sites on the HA stem have been targeted by antibodies previously, including epitopes recognized by the broadly neutralizing antibodies A06[7,8], CR6261[9,10], F10[11], CR8020[12] and FI6[13] Several recent studies have suggested that stem antibodies may be present in a significant number of individuals [14,15], and the ability to re-elicit stem antibodies by immunization [16] has raised hopes that a universal vaccine for influenza A may be achievable. While such antibodies against the stem are highly cross-reactive, most antibodies that target the more variable receptor binding domain (RBD) of HA1 exhibit limited breadth of neutralization. Crystal structures reveal that, although a few antibody footprints on the HA1 RBD sometimes coincide with the receptor binding site [17–20], many of the essential interactions are made with hypervariable regions well outside of the functionally conserved region involved in sialic acid recognition[21,22]. However, recent work suggests that some rare antibodies against the HA1 RBD can achieve modest cross-reactivity[20,23,24]. Thus, identification and structural understanding of heterosubtypic antibodies against the RBD with broad activity especially against human pandemic viruses (H1, H2, and H3 subtypes) would be a major advance and facilitate development of new therapeutics complementary to those targeting the stem. Here we report the functional and structural characterization of one such antibody, C05, which neutralizes multiple subtypes by inserting an extended CDR loop into the receptor binding pocket.

Isolation and characterization of C05

Previously, we isolated antibodies from phage-displayed combinatorial libraries derived from Turkish patients who survived H5N1 avian flu infection[7,8]. and identified a novel class of antibodies effective against a broad range of group 1 influenza A viruses. Here, we

utilized a similar approach to identify antibodies that would neutralize both group 1 and group 2 viruses. Phage libraries constructed from the immune repertoires of seasonal influenza infection survivors were doubly selected against HA proteins from H1 (group 1) and H3 (group 2). This process yielded a limited number of clones that reacted broadly with both H1 and H3 HA proteins. One clone, C05, which utilizes the V_H3-23 and V_K1-33*01 heavy and light chain V-genes, respectively, has two distinctive structural features: a long 24 amino-acid heavy chain HCDR3 (Supplementary Fig. 1) and a 5-residue somatic insertion in HCDR1. C05 potently neutralizes viruses from H1, H2, H3, and H9 subtypes, *in vitro* (Fig. 1 and Table 1a), including the influenza A subtypes which have caused human pandemics. However, C05 had no detectable activity against H5, as well as some of the H1 viruses tested. In sharp contrast to most broadly neutralizing antibodies to flu[9–11,25], which bind the more conserved stem region, C05 inhibits receptor binding and hemagglutination (Table 1a), suggesting recognition of an epitope in the HA1 globular head domain.

Protection in vivo

To explore the in vivo efficacy of C05, we examined its ability to protect mice from lethal challenge with H1N1 or H3N2 viruses. When administered prophylactically 24 hours before challenge with A/Memphis/3/2008 (H1N1) virus, 1 mg/kg C05 IgG protected 100% of mice from death and prevented substantial weight loss (Fig. 2a). Lower doses (0.25 to 0.025 mg/kg) still afforded proportional protection. For A/Aichi/2/X-31/1968 (H3N2) virus, a 10 mg/kg dose protected 100% mice from death and both 1.0 and 0.25 mg/kg doses afforded protection for the majority (Fig. 2b).

Next we wished to determine the C05 therapeutic potential against an established H1N1 or H3N2 infection. A single 15 mg/kg IgG dose was administered at 1,2,3,4, or 5 days after lethal challenge with A/Memphis/3/2008 (H1N1) or A/Aichi/2/X-31/1968 (H3N2) viruses. In both instances, mice treated up to 3 days post-infection were completely protected (Fig. 2c, d). We then evaluated the minimal dose needed to overcome established infection 3 days post-inoculation, the latest time at which C05 treatment was completely protective against death. As little as a single 3 mg/kg dose of antibody prevented infection-related death in 80% of the animals (Supplementary Fig. 2). In aggregate, these in vivo results suggest utility of C05 in both prevention and treatment.

Avidity is critical for C05 function

To further profile its breadth of activity, we tested Fab C05 binding to a large panel of HAs by biolayer interferometry (BLI), including representative members of most of the 16 subtypes. Fab C05 binds to a number of diverse HAs spanning both group 1 and group 2 viruses, including members of H1, H2, H3, H9, and H12 subtypes (Table 1b). Surprisingly, many HAs from viruses neutralized by IgG C05 are bound with only intermediate-to-low affinity by the Fab (K_d ~ 100 nM-10 uM), well outside the range typically required for effective neutralization, such as by stem antibodies (K_d < 100 nM)[10,12]. To confirm these unexpected results, we selected four HAs from neutralized viruses that bound C05 Fab with a range of affinities (K_d = 18, 430, 720 nM, and one with no detectable Fab binding by BLI) and assessed C05 binding in solution by isothermal titration calorimetry (ITC). The ITC results were in good agreement with the K_d, measured by BLI (Table 1c). Remarkably, although only very weak binding (K_d~10uM) of C05 Fab to A/Brisbane/10/2007 (H3N2) HA was detected by ITC (undetectable by BLI), the corresponding virus was neutralized by C05 IgG in vitro (Table 1c). Thus, despite the unusually low affinity of C05 Fab for many of its targets, C05 IgG potently neutralizes virus replication in vitro and is protective in vivo. To the best of our knowledge, only one other neutralizing antibody has been reported with such a striking discrepancy between binding affinity and neutralization. Broadly neutralizing anti-HIV antibody 2G12 binds a high mannose glycan cluster on the gp120 subunit of the

HIV surface spike, but its affinity for a single high mannose glycan is very low (K_d ~ μM)[26]. However, a highly unusual domain swapping of the Fabs allows 2G12 to bind multiple glycans simultaneously and thereby achieve high affinity binding (nM) through avidity[27]. For C05, the presence of multiple antibody binding sites on each trimeric HA spike and the high density of HA on the virus surface may facilitate simultaneous engagement of both arms of the C05 IgG, resulting in much higher avidity compared to Fab. EM experiments with H1, H2, and H3 HAs show that 3 C05 Fabs are bound per trimer (Fig. 3f), but their geometry is inconsistent with bivalent attachment by an IgG. Indeed, C05 IgG binds to an array of immobilized HA with much higher affinity (nM to ~pM) than its Fab, consistent with the single particle EM analysis confirming the ability of IgG to cross-link HA spikes (Supplementary Fig. 3). Thus, some antibodies with low affinity Fab interactions can still have significant activity *in vitro* and *in vivo* and may represent an under-appreciated component of the immune repertoire. The role of avidity may be more or less pronounced depending upon the nature of the epitope and the density of the antigen on the viral surface, with clustered epitopes, such as those on the HAl RBD, benefiting most from avidity, while sterically crowded (e.g., HA stem) or sparse epitopes (HIV Env spikes) likely prevent bivalent binding. In the latter case, high affinity binding must be achieved by the Fab or by heteroligation of two different antigens, which may play a more prominent role in neutralization of human viruses, such as HIV[28].

Crystal structure of C05 complex with HA

To understand how antibody C05 achieves heterosubtypic neutralization, we determined the crystal structure of C05 Fab in complex with the HAl subunit from the A/Hong Kong/1/1968 (HK68/H3) at 2.95Å resolution, and Fab C05 in complex with the complete, trimeric ectodomain of HK68/H3 at 4.25Å (Supplementary Table 1). In addition, high resolution structures of HK68/H3 HA (1.90 Å) and C05 Fab (2.30 Å) provided high quality starting models for refinement of the complexes. Few differences are apparent between the isolated HA1 and the HA1 subunit in trimeric HA, as in other HA1 crystal structures[18]. Further, the C05-HA1 and C05-HA trimer structures are in excellent agreement (Supplementary Fig. 4), indicating the C05-HA1 complex faithfully recapitulates the native interaction.

Three C05 Fabs bind near the membrane-distal end of the HA trimeric spike (Fig. 3a), and HCDR3 penetrates the receptor binding site (Fig. 3b). Several striking features of the C05 interaction are immediately apparent. C05's exceptionally long, 24-residue HCDR3 dominates the antibody-antigen interaction (Fig. 3b). While ~1.5% of human antibodies in the Abysis database have an HCDR3 of 24 or more residues, only 3 of the over 1000 Fab structures in the Protein Data Bank (PDB) have more than 24-residue HCDR3s (Supplementary Fig. 5). Very long CDRs can adopt unusual conformations, such as the "hammerhead" structure in PG9/PG16[4,6,29], and these long loops are presumably crucial for antigen recognition, yet few structures of such antibodies bound to antigen have been reported. The C05 structure, therefore gives us a valuable glimpse at how long HCDR3s can be used to target recessed or evolutionarily constrained epitopes.

C05's long HCDR3 extends far from the antibody surface, with its most distal end forming a β-hairpin. The long HCDR3 holds the V_H and V_L domains at a distance from the HA surface (Fig. 3c), preventing the light chain from contacting the epitope, reminiscent of the heavy-chain dominant recognition by stem-directed, V_H1-69 antibodies[9,11]. To a first approximation, C05 HCDR3 resembles the PG9/PG16 hammerhead, but with its shorter C-terminal branch truncated (Supplementary Fig. 6). The HCDR3 β-hairpin inserts into the shallow HA receptor binding pocket near the HA spike apex (Fig. 3d). HCDR3 overlaps with the binding site for glycan receptor and suggests that C05 inhibits virus attachment by direct competition with sialic acid (Fig. 3e). However, C05 interaction with the receptor binding site differs significantly from sialic acid binding to HA.

Aside from HCDR3, only HCDR1 makes additional minor interactions with HA, in part due to a 5-residue somatic insertion (Fig. 3g and Supplementary Fig. 1). Insertions and deletions (indels) within the V-gene encoded region are relatively rare [30,31], but recent work suggests that these indels may be selected during affinity maturation and can be important for antibody function[32,33]. Consistent with the minor contacts made by HCDR1, removal of the 5-residue insert [del(FGEST)] or scanning mutagenesis of HCDR1 had no detectable effect on C05 binding to HK68/H3 and several other H1, H2, and H3 HAs (Table 2 and Supplementary Table 2), whereas binding of C05-del(FGEST) to H3 Perth09 HA was reduced nearly l00-fold compared to wild-type C05 (Table 2), suggesting that HCDR1 may make additional interactions with Perth09 (see discussion in Supplementary Information and Supplementary Fig. 7). Thus, the HCDR1 insertion is dispensable for binding to most HAs tested, where the HCDR3 loop alone is sufficient for full activity. However, nearby antibody CDRs and framework regions likely contribute to binding by supporting HCDR3, as the loop conformation is essentially identical in the crystal structure of C05 Fab alone. In particular, the tip of HCDR2 interacts with the backside of the HCDR3 loop and harbors several somatic mutations that may have arisen to best position and stabilize HCDR3 for HA binding (Supplementary Fig. 8). In contrast, HCDR1 appears to play a lesser role, as the above mutations above did not prevent C05 binding.

Loop-insertion binding mechanism

Despite high sequence diversity immediately surrounding the receptor binding site, the functional constraints imposed by binding to sialic acid receptors restrict variation within the pocket itself. Thus, while other antibodies can bind in or near the receptor binding site, a typical antibody footprint would extend well beyond the conserved functional region and contact at least some variable positions around the receptor binding site, rendering them largely strain specific and susceptible to escape through antigenic drift. A notable exception is CH65, which cross-neutralizes an unusually large subset of H1N1 viruses, but not other subtypes[20]. However, unlike C05, CH65 binds HA using both heavy and light chains (including 5 of the 6 CDR loops), which increases contact with these more variable surfaces (Supplementary Fig. 9). In contrast, C05's long HCDR3 targets the conserved elements of the receptor binding site, and enters and exits the pocket without contacting many of the surrounding variable positions (Fig. 4a, b). Indeed, we were unable to generate C05 escape mutants with an H3 virus despite repeated attempts.

Loop insertion is a common mechanism for achieving high affinity protein-protein interactions, as illustrated notably by BPTI[3]. Due to the restricted, single CDR-driven interaction of C05 with HK68/H3 HA, only 550 $Å^2$ of surface area is buried on the HA by C05, which is unusually small for a protein antibody-antigen interaction. This small footprint allows C05 to achieve broader cross-reactivity compared to other antibodies that extend their interface outside of the receptor binding site (Supplementary Table 3, e.g., ~650 $Å^2$ buried surface on HA for CH65 and 740 $Å^2$ for 2D1). Single particle 3D EM reconstructions of C05 bound to H1, H2, and H3 HAs (Fig. 3f, Supplementary Fig. 10), along with binding experiments probing the effect of several mutations in the HCDR3 loop (Supplementary Fig. 11), clearly illustrate that binding to other subtypes is likely very similar to that in the H3 crystal structure.

Epitope conservation and variation correlating with escape

The wide range of affinities for C05 against a panel of HAs suggests that epitope variation has a significant impact on C05 activity. Therefore, we examined sequence diversity contained within all full-length, non-redundant human H1, H2, and H3 HA sequences in the NCBI FLU database[34]. An analysis including all 16 virus subtypes yielded similar results (Supplementary Table 4). Of 17 C05 contact residues on HA, 6 core residues are ≥99%

conserved across human H1, H2, and H3 viruses, including 98, 134, 136, 153, 190, and 194 (Fig. 4a, b). The remaining 11 positions are generally <50% conserved (ranging from 42–76%). Therefore, the C05 epitope is markedly less conserved (mean % identity/mean % conservation across all contact residues is 59%/64%) compared to stem epitopes recognized by bnAbs (76%/86% for CR6261 and 71%/80% for CR8020) due to greater variation within the receptor binding site. Thus, the range of observed affinities for C05 binding to H3 HAs may arise from multiple, subtle mutations (increasing Kd 2–10 fold) that in combination reduce binding below the threshold of detection. Substitutions at HA1 190,225,226, and 228 are important for determining receptor specificity in HAs adapted to particular hosts (e.g., α2–3 vs. α2–6 sialoglycans for avian vs. human viruses, respectively) and mutations modulating receptor affinity are a well-documented mechanism of antibody escape[35]. C05 makes only minor contacts with Leu226 and does not contact 225 or 228. C05 interacts more extensively with Asp190 in HK68/H3, but Asp, Glu, and Val are present at position 190 in our panel of HAs bound by C05. Thus, C05 may bind equally well to HAs with either α2,3 or α2,6 receptor specificity, but variability within the receptor binding site may account for some of the observed heterogeneity in C05 binding.

Several common insertions and deletions (indels) are close to the receptor binding site and may impact antibody binding (Supplementary Fig. 12). Insertions at position 133a result in a local bulge that clashes directly with C05 HCDR3 and likely abrogates binding. This insertion is observed in 100% of all H6 and H10, 96% of all H5 and 66% of all H1 sequences. Consistent with this observation, no H5 viruses tested were neutralized and binding to H6, H10, and multiple H5 isolates was undetectable, even with 10 uM IgG. Similarly, C05 binding to 5 different H1 HAs with the 133a insertion was undetectable with 10 uM IgG, and only very weak binding was observed to a sixth (A/Singapore/6/1986(H1N1)); no viruses with the insertion were neutralized. In contrast, all H1 HAs without the 133a insertion were bound and/or neutralized by C05. Thus, the 133a insertion appears to negatively impact binding of C05, similar to the effect of the 133a insertion on CH65[20]. In addition, indels near position 158 and the 220-loop correlate with poor activity against H4, H6, H7, H10, HI4, and HI6 subtypes (Supplementary Fig. 12). These insights have enabled us to delineate the most important structural requirements for high affinity, cross-reactive binding to the receptor binding site.

Implications for anti-viral therapeutics and vaccine strategies and design

Because C05 binding is exclusively accomplished through the heavy chain, and primarily via HCDR3, its interaction with HA defines a minimal set of contacts sufficient for cross-group neutralization, which may be exploited to develop antiviral therapeutics. The ability of a bnAb, such as C05, to penetrate the shallow receptor binding site with relatively high affinity (μM to nM) and avidity (nM) compared to its natural receptor (mM) makes such an antibody extremely attractive for therapeutics and diagnostics. C05 was discovered from a single human donor source library using the power of phage display library technology to isolate this rare antibody binding interaction. Due to the combinatorial nature of antibody library construction, we cannot explicitly determine whether the C05 heavy chain and light chain pairing previously existed in the donor or not. However, other receptor binding site antibodies, such as CH65[23], have been isolated from B-cells showing that receptor binding site antibodies can be found naturally and are potentially inducible by vaccination strategies. Thus, design of HA immunogens to elicit more broadly neutralizing head antibodies may now be more feasible and will complement the arsenal of already promising stem antibodies for use in a more universal vaccine, as well as in structure-based and computational approaches to design small proteins and other possible therapeutics against flu, such as already achieved against the stem epitope[36].

METHODS SUMMARY

Isolation of C05

Phage antibody libraries were cloned from the bone marrow from donors with confirmed influenza virus exposure. Phage were selected by sequential panning against A/Wisconsin/67/05 (H3N2) followed by A/New Caledonia/20/1999 (H1N1).

Neutralization

Microneutralization and hemagglutinin inhibition assays were carried out according to standard protocols, as described in detail in the Methods.

In vivo protection in mice

Animal experiments were performed in accordance with the guidelines of the Mount Sinai School of Medicine and St. Jude Children's Research Hospital Institutional Animal Care and Use Committees (IACUC). All animal experiments were done essentially as described in[8]. Virus strains used in these studies were A/Memphis/3/2008 (H1N1) and A/Aichi/1/X-31/1968 (H3N2). 5–6 week old BALB/c mice were used for the H1N1 studies and 8-week old DBA/2 mice for the H3N2 studies.

Proteins

Antibodies were expressed in *E. coli*, baculovirus, and mammalian cells as described in the Methods. HAs were expressed in baculovirus as previously described[12] or purchased from Protein Sciences Corp.

Binding Data

Binding of C05 IgG or Fab to recombinant HAs and K_d, determination was performed by biolayer interferometry, isothermal titration calorimetry, and ELISA.

Structure determination

Robotic crystal screening was carried out using the Rigaku Crystalmation system at the Joint Center for Structural Genomics. Diffraction data were collected at the APS GM/CA-CAT 23ID-B and 23ID-D, and SSRL 11-1 beam-lines and processed using HKL2000 (HKL Research) and XPREP (Bruker). Structures were solved by molecular replacement using Phaser, adjusted using Coot, and refined in Phenix. Kabat numbering was applied using Abnum[37]. Structural analyses were performed using MS and CONTACSYM.

Sequences

PDB antibody sequences were analyzed through the Abysis database.). Hemagglutinin sequence datasets were downloaded from the NCBI FLU database[34], aligned with Muscle[38], and analyzed using GCG (Accelrys) and custom shell scripts.

Full methods and any associated references are available in the online version of the paper at www.nature.com/nature.

Methods

Serology: HA protein and whole virus ELISA

Recombinant HA proteins: H5 protein A/Vietnam/1203/2004 (Protein Sciences)-10ng/well; recombinant HA H1 protein A/New Caledonia/20/99 (Protein Sciences)-10ng/well; recombinant HA H3 protein A/Wisconsin/67/05 (Protein Sciences)-10 ng/well; H1N1

virusA/New Caledonia (Bio-Source)-70ng/well; H3N2 virus A/Panama/2007/99 (BioSource)-10ng/well.

ELISA plates were coated as indicated with either recombinant HA protein or inactivated virus incubated overnight at room temperature. The next day plates were blocked (1% bovine serum albumin in PBS/0.05% Tween-20) and then 0.1 ml serum samples, diluted in blocking buffer, were incubated, washed, and detected using a peroxidase conjugated anti-human Fc antibody (Jackson Immuno) and TMB detection (BioFX). Absorbance at 450nm was read, data recorded, and reported herein.

Library construction

Antibody phage display libraries were created from the individual immune repertoires of confirmed influenza infection survivors. Bone marrow aspirates were collected and stored in RNALater (Ambion) to preserve RNA integrity until processing for library construction. Serum samples were taken from each individual and used to confirm antibody reactivity to various HA proteins or inactivated influenza viruses by ELISA (Supplemental Fig. 13). The phage display libraries were constructed as previously described[7].

Selection of HA binding clones

Phage antibody library panning was done essentially as described[7]. Cross-reactive antibodies were identified by selection on both H3 and H1 HA protein antigens. After two rounds of panning on H3 HA A/Wisconsin/67/05, H1 HA protein from A/New Caledonia/20/1999 replaced the H3 HA protein for two additional rounds. A fifth, and final, round of selection was performed on the H3 HA protein.

IgG expression and Fabs

The C05 heavy chain and light chain regions were mammalian codon optimized, synthesized (GeneArt) and cloned into the pTT5-based expression vectors. Expression was done essentially as described in[7]. C05 Fab fragment was obtained by Lys-C digestion of IgG, followed by purification by protein A (GE Healthcare), protein G (GE Healthcare), cation exchange (MonoS, GE Healthcare), and gel filtration (Superdex200, GE Healthcare). For binding studies, C05 Fab was expressed recombinantly using the baculovirus system. A DNA fragment derived from the promoter region of pFastBacDual (Invitrogen) was fused to the gp67 and the honey bee mellitin (HBM) signal peptides by overlap PCR, yielding a fragment with head-to-head p10 and polyhedrin promoters upstream of the HBM and gp67 signal peptides, respectively (i.e., HBM-p10-pPolyH-gp67). C05 Fab heavy and light chain regions were synthesized (GenScript), fused to the promoter-signal peptide cassette by overlap PCR (heavy chain downstream of pPolyH-gp67 and light chain downstream of p10-HBM), and ligated into the SfiI sites of a derivative of pFastBacDual. A His_6-tag was introduced at the C-terminus of the light chain to facilitate purification.

Mutations to probe the importance of the CDR H1 insertion were generated by site-directed mutagenesis using the QuikChange Multi Lightning kit (Agilent). The resulting baculovirus transfer vectors were used to generate recombinant bacmids using the Bac-to-Bac system (Invitrogen) and virus was rescued by transfecting purified bacmid DNA into Sf9 cells using Cellfectin II (Invitrogen). C05 Fab proteins were produced by infecting suspension cultures of Hi5 cells (Invitrogen) with recombinant baculovirus at an MOI of 5–10 and incubating at 28°C shaking at 110 RPM. After 72 hours, the cultures were clarified by two rounds of centrifugation at 2000g and 10,000g at 4°C. The supernatant, containing secreted, soluble Fab was concentrated and buffer exchanged into 1× PBS, pH 7.4. After metal affinity chromatography using Ni-NTA resin, Fabs were purified by protein G affinity chromatography (GE Healthcare) and gel filtration (Super-dex200, GE Healthcare).

ELISA

Microtiter plates were coated with 0.1 ml of the following HA antigens diluted in coating buffer and incubated overnight at room temperature: 100 ng/ml H5N1 Vietnam 1203/04, 700 ng/ml H1N1 New Caledonia/20/99, and 100 ng/ml H3N2 Wisconsin/67/05. Blocking was done with 0.3 ml of blocking buffer (4% non-fat dry milk in PBS/0.05% Tween-20). Following blocking, antibodies were diluted to 0.5 μg/ml in 2% non-fat dry milk blocking buffer were incubated for two hours at 4C, washed, and later detected using a 1:3000 dilution of peroxidase conjugated anti-human F_c, antibody (Jackson ImmunoResearch) in 2% non-fat dry milk blocking buffer and standard TMB substrate detection (BioFX). Absorbance at 450nm was read, data recorded, and reported herein.

Viruses

Recombinant influenza viruses were generated using reverse genetics as previously described[39]. Briefly, 1ug each of 10 plasmids was transfected into 293 T cells in monolayer. Each transfection contained ambisense plasmids (for the expression of both vRNAs and mRNAs) for the A/Puerto Rico/8/34/PA, PB1, PB2, NP, M, and NS segments, in addition to vRNA (pPOL1 type) and protein expression plasmids (pCAGGS type) for A/Adachi/X-31/1968 HA and NA (pCAGGS expression plasmid was kindly provided by J. Miyazaki, Osaka University, Osaka, Japan)[40]. Twenty hours following transfection, 293T cells were resuspended in cell culture supernatant, and used to inoculate 10-day-old embryonated eggs.

Microneutralization

Antibodies were screened for neutralizing activity against viruses as follows. Two fold serial dilutions of each mAb were incubated with 100 $TCID_{50}$ of virus in PBS at 37°for 1 h. Madin-Darby Canine Kidney cell monolayers in 24 well plates were washed once with PBS and inoculated with virus-antibody mixtures. Following incubation for 1 hr at 37°C in 5% CO_2, the inoculum was removed and monolayers were again washed once with PBS. Opti-MEM supplemented with 0.3% BSA, 0.01% FBS and 1ug/ml TPCK-treated trypsin was added and cells were incubated for 72 h at 37°C. The presence of virus in cell culture supernatants was assessed by HA assays using 0.5% chicken red blood cells.

Hemagglutination inhibition

Hemagglutination inhibition titers were determined using 4 hemagglutinating units of HA protein or virus. HA protein or virus was incubated for 1 hour at room temperature with serial two-fold dilutions of C05 IgG in 96-well, V-bottom microtiter plates (Costar) followed by addition of 0.5% chicken red blood cells and mixing. The mixture was incubated for 30 minutes at room temperature followed by brief centrifugation at 1000 RPM to pellet the red blood cells.

Generation of escape mutants

Briefly, H3N2 A/Aichi/1/X-31/1968 virus was incubated with a neutralizing excess of monoclonal antibody for 45 minutes at room temperature. The virus-mAb mix was inoculated into 10 day old embryonated eggs and incubated at 37°C for 48 hrs. Eggs were inoculated in triplicate. The virus (allantoic fluid) grown under these conditions was harvested and tested for virus outgrowth by HA assay. No viral growth was observed by hemagglutination of chicken red blood cells. The experiment was performed twice.

In vivo protection

Animal experiments were performed in accordance with the guidelines of the Mount Sinai School of Medicine and St. Jude Children's Research Hospital Institutional Animal Care and Use Committees (IACUC). All animal experiments were done essentially as described in[8].

Virus strains and titers used in these studies were H1N1 A/Memphis/3/2008 (25MLD_{50}, 10^5 EID_{50}) and H3N2A/Adachi/1/X-31/1968 (33MLD50, 300 PFU). Mice were 5–6 week old Balb/C for the H1N1 studies and DBA/2 for the H3N2 studies.

Cloning, expression and purification of influenza A hemagglutinins

Based on H3 numbering, cDNAs corresponding to residues 11–329 (HAl) and 1–176 (HA2) of the influenza A HA ectodomain were fused to an N-terminal gp67 signal peptide and to a C-terminal biotinylation site (amino acid sequence: GGGLNDIFEAQKIEWHE), trimerization domain, and His_6-tag by overlap PCR, essentially as previously described[12]. The trimerization domain and His_6-tag were separated from the HA ectodomain by a thrombin cleavage site. In the case of the HK68/H3 trimer construct used for crystallization, the biotinylation site was omitted from the construct. For the HK68/HA1 subunit used for crystallization, HA1 residues 43–309 were fused to the gp67 signal peptide (N-terminus) and a C-terminal His_6-tag. The resulting PCR products were digested with SfiI and inserted into a custom baculovirus transfer vector (pDCE198). The production of virus and expression conditions were essentially as above for the C05 Fabs. After metal affinity chromatography using Ni-NTA resin, trimeric HAs for crystallography were digested with trypsin (New England Biolabs, 5mU trypsin per mg HA, 16 hours at 17°C) to produce uniformly cleaved (HA1/HA2), and to remove the trimerization domain and His-tag. After quenching the digests with 2mM PMSF, the digested material was further purified by anion exchange chromatography (10mM Tris, pH 9.0, 50–1M NaCl) and size exclusion chromatography (10mM Tris, pH 8.0, 150mM NaCl).

Expression and purification of BirA

E. coli biotin ligase (BirA enzyme) was expressed and purified in a manner similar to previous reports[41], but with an N-terminal His tag, essentially as previously described[12]. Briefly, a pET21a derivative containing the *E. coli birA* gene (pDCE095) was transformed into BL21(DE3) cells, grown in shake flasks in low salt LB medium at 37°C to an OD (600nm) of ~0.7, then shifted to 23°C and induced with the addition of isopropyl-beta-D-thiogalactopyranoside (IPTG) to a final concentration of 1mM. The culture was incubated at 23°C for ~16 hours after induction. The cells were lysed and homogenized by two passes through an EmulsiFlex C-3 cell disruptor (15kPSI), and birA was purified by Ni-affinity (NiNTA resin, Qiagen), anion exchange (MonoQ column, GE Healthcare), and gel filtration. Purified BirA protein was concentrated down to 5mg/mL in 50mM Tris, pH 7.5, 200mM potassium chloride, 5% glycerol, aliquoted, flash frozen in liquid nitrogen, and stored at −80°C.

Biotinylation and purification of influenza HAs for binding studies

After expression and Ni-NTA purification of influenza A HA, as described above, proteins for binding studies were concentrated down to ~2–5mg/mL total protein. The HAs were biotinylated by the addition of 25μg BirA enzyme/mg total protein, in a buffer of the following composition: 100mM Tris pH 8.0, 10mM ATP, 10mM MgOAc, 50μM biotin, with less than 50mM NaCl. The biotinylation reactions were incubated at 37°C for 1–2 hours. Biotinylated HAs were purified by size exclusion chromatography, and concentrated to ~5–20 mg/mL.

K_d determination by bio-layer interferometry

K_d's were determined by bio-layer interferometry (BLI) using an Octet Red instrument (ForteBio, Inc.). Biotinylated HAs, purified as described above, were used for these measurements. HAs at ~10–50 μg/mL in 1× kinetics buffer (1× PBS, pH 7.4,0.01 % BSA, and 0.002% Tween 20) were loaded onto streptavidin coated biosensors and incubated with

varying concentrations of CR9114 Fab in solution. All binding data were collected at 30°C. The experiments comprised 5 steps: 1. Baseline acquisition (60 s); 2. HA loading onto sensor (300–600 s); 3. Second baseline acquisition (180–200 s); 4. Association of C05 for the measurement of k_{on} (180 s); and 5. Dissociation of C05 for the measurement of k_{off} (180 s). 4–6 concentrations of C05 were used, with the highest concentration varying, depending on the HA affinity, from 50 to 1000nM. Baseline and dissociation steps were carried out in buffer only. The ratio of k_{on} to k_{off} determines the K_d reported here. The sequences of all proteins used in this work are available in Fasta format at the end of this document. All binding traces and curves used for fitting k_{on} and k_{off} are reported in Supplemental Figs. S14 and S15.

K_d determination by isothermal titration calorimetry

Isothermal titration calorimetry (ITC) was performed using an ITC_{200} calorimeter (Microcal). All proteins were dialyzed extensively against PBS buffer prior to the titrations. The experiments were performed at 25 °C. A typical titration consisted of injecting 1.6 μl, aliquots of C05 Fab (0.5 mM) into 70 μM HA solution in the cell at time intervals of 90s to ensure that the titration peak returned to the baseline. ITC data were corrected for the heat of dilution by subtracting the mixing enthalpies for titrant solution injections into protein-free buffer. ITC data were analyzed using program Origin (Version 7.0) as provided by the manufacturer. We used a single set of identical binding sites model.

Due to the high molecular weight of the system and the very poor expression of the A/Brisbane/10/2007 (H3N2) HA, we were unable to achieve a high enough molar concentration of HA in the ITC cell to obtain a complete, high quality titration curve. For a K_d of 10 uM, the manufacturers guidelines suggest 0.5 mM HA in the cell and 5 mM Fab in the syringe. This would correspond to ~30mg/mL HA (~10mg total) and ~250mg/mL Fab (~20mg total). However, we were only able to obtain ~1mg of the A/Brisbane/10/2007 (H3N2) HA from 10L of insect cell culture, precluding the possibility of obtaining the quantity of protein required for an optimal experiment. In addition, while C05 Fab could be obtained in good yields and could be concentrated to at least 50mg/mL (~1mM), clear self-association between C05 molecules was apparent even at ~19mg/mL (~0.38 mM), the concentrations used in the experiment reported here. However, after subtraction of Fab injections into a buffer filled cell to correct for the heat of dilution resulting from the Fab self- association at high concentrations, the resulting data could still be fit reasonably well and an approximate value for the K_d could be obtained. See Supplemental Fig. 16.

Electron microscopy of C05 Fab with H1, H2, and H3 HAs

Negative stained grids were prepared by applying 0.1 mg/ml of the purified complex to a freshly glow discharged carbon coated 400 Cu mesh grid and stained with Nano-W. Grids were viewed using a FEI Tecnai TF20 electron operating at an accelerating voltage of 120kV and imaged at a magnification of 100,000×. Images were acquired on a Gatan 4kx4k CCD camera in 5-degree tilt increments from 0 to 55~ using a defocus range of 700 to 900 nm. The tilt angles provided additional particle orientations to improve the image reconstruction. The pixel size of the CCD camera was calibrated at this magnification to be 1.09Å using a 2D catalase crystal with known cell parameters.

Image processing

For each complex, particles were automatically selected from micrographs using the DoG Picker software through the Appion packagev[42,43]. The contrast transfer function estimation for micrographs was completed using ctffind3 and ctfttilt[42,44]. Particles were binned by 4 (80×80 sized boxes) and reference free 2D class averages were calculated using the Sparx package, without imposing symmetry[45]. An unliganded 25Å hemagglutinin (H1) volume

generated with Sparx was used as the initial model for the image reconstruction process, with the reference free class averages as the experimental images. Density for the Fabs could be visualized after 3 cycles of refinement. Refinement was continued for 70 cycles with decreasing angular search parameters. The resultant model was then used as the initial model for the iterative image reconstruction process against the raw particles binned by 2 (160×160 sized boxes). CTF correction was applied during this procedure using the Sparx package. C3 symmetry was imposed throughout the image reconstruction process. The final 3D image reconstructions have an estimated resolution of 17Å according to an FSC of 0.5.

Model fitting

Coordinates of A/Solomon Islands/312006 (HINI), A/Japan/30S/19S7 (H2N2) in addition to C05 were fitted into the respective EM reconstructions. For H3, the coordinates of A/Hong Kong/1/1968 (H3N2) were used in the EM reconstruction of A/Perth/16/2009 (H3N2) with C05 Fab. The automated fit of each component was manually improved via rigid body movement using the program UCSF Chimera to minimize the number of clashes between HA and the Fabs while maintaining the highest possible correlation coefficient value with the Chimera Fit tool. This resulted in a portion at the base of the stem region of HA being excluded from the image reconstruction. Coincidentally, this region of HA possesses high B-factors in the crystal structures and may adopt distinct conformations on the EM grid. The density for this region can be seen at lower contour thresholds.

Crystallization and structure determination of the HK68/H3 HA

Gel filtration fractions containing HK68/H3 HA were concentrated to ~9mg/mL in 10mM Tris, pH 8.0 and 50mM NaCl. Initial crystallization trials were set up using the automated Rigaku Crystalmation robotic system at the Joint Center for Structural Genomics (www.jcsg.org). The crystal used for data collection was grown by the sitting drop vapor diffusion method with a reservoir solution (200 μl.) containing 2.0M ammonium sulfate, 100mM sodium cacodylate pH6.5, and 200mM NaCl. Drops consisting of 100 nL protein + 100 nL precipitant were set up at 20°C, and crystals appeared within 3–7 days. The resulting crystals were cryoprotected by brief immersion in well solution supplemented with 35% glycerol then flash cooled and stored in liquid nitrogen until data collection.

Diffraction data for the HK68/H3 HA were collected on beamline 11–1 at the Stanford Synchrotron Radiation Lightsource (SSRL). The data were indexed in space- group $C222_1$, integrated, and scaled using HKL2000 (HKL Research). The structure was solved by molecular replacement to 1.90 Å resolution using Phaser[46]. A protomer from 2VIU[18] (A/Aichi/2/X-31 (H3N2) HA) was used as the initial search model and 3 copies (forming a non-crystallographic trimer) were found in the asymmetric unit. At this point, poorly defined regions of the model were trimmed and the HA was mutated *in silica* to match the HK68/H3 sequence. Rigid body refinement, simulated annealing and restrained refinement (including TLS refinement, with one group for each HA1 or HA2 domain) were carried out in Phenix[47]. Riding hydrogens were used during refinement and are included in the final model. Between rounds of refinement, the model was built and adjusted using Coot[48]. Waters were built automatically using the "ordered_solvent" modeling function in Phenix[47]. Refinement statistics can be found in Supplementary Table 1.

Crystallization and structure determination of the C05 Fab

Gel filtration fractions containing the C05 Fab were concentrated to ~11 mg/mL in 10mM Tris, pH 8.0 and 50mM NaCl. Initial crystallization trials were set up using the automated Rigaku Crystalmation robotic system at the Joint Center for Structural Genomics (www.jcsg.org). Several hits were obtained, with the most promising candidates grown in ~2.0–2.5M ammonium sulfate between pH 5 and 7. Optimization of these conditions

resulted in diffraction quality crystals. The crystals used for data collection were grown by the sitting drop vapor diffusion method with a reservoir solution (1mL) containing 1.8M ammonium sulfate, 100mM sodium acetate pH 5.4, and 50mM NaCl. Drops consisting of 0.5μL protein + 0.5μL precipitant were set up at 4°C, and crystals appeared within 3–7 days. The resulting crystals were cryoprotected by soaking in well solution supplemented with increasing concentrations of ethylene glycol (5% steps, 1hr/step), to a final concentration of 20%, then flash cooled and stored in liquid nitrogen until data collection.

Diffraction data for the C05 Fab crystals were collected on the GM/CA-CAT 23ID-D beamline at the Advanced Photo Source at Argonne National Laboratory. The data were indexed in spacegroup $P4_12_12$, integrated, scaled, and merged using HKL2000 (HKL Research). The structure was solved by molecular replacement to 2.30 Å resolution using Phaser[46]. PDB codes 1AQK and 1VGE were used as search models for the variable and constant domains, respectively, and 2 complete Fabs were found in the asymmetric unit. Rigid body refinement, simulated annealing and restrained refinement (including TLS refinement, with one group for each Ig domain) were carried out in Phenix[47]. Riding hydrogens were used during refinement and are included in the final model. Between rounds of refinement, the model was built and adjusted using Coot[48]. Waters were built automatically using the "ordered_solvent" modeling function in Phenix[47]. Refinement statistics can be found in Supplementary Table 1.

Crystallization and structure determination of the COS-HK68/H3 HA1 complex

Gel filtration fractions containing the C05-HK68/H3 HA1 complex were concentrated to ~9mg/mL in 10mM Tris, pH 8.0 and 50mM NaCl. Initial crystallization trials were set up using the automated Rigaku Crystalmation robotic system at the Joint Center for Structural Genomics (www.jcsg.org). The crystals used for data collection were grown by the sitting drop vapor diffusion method with a reservoir solution (200 μl.) containing 10% (w/v) PEG 3000, 200mM zinc acetate, 100mM sodium acetate pH 4.5. Drops consisting of 100 nL protein + 100 nL precipitant were set up at 4°C, and crystals appeared within 3 days and continued to grow larger until approximately day 7. The resulting crystals were cryoprotected by brief immersion in well solution supplemented with 30% ethylene glycol, then flash cooled and stored in liquid nitrogen until data collection.

Diffraction data for the C05-HK68/H3 HA1 complex were collected on the GM/CA-CAT 23ID-D beamline at the Advanced Photo Source at Argonne National Laboratory. The data were indexed in spacegroup $P2_1$, integrated, scaled, and merged using HKL2000 (HKL Research). The structure was solved by molecular replacement to 2.95 Å resolution using Phaser[46]. The isolated HA1 subunit from the HK68/H3 structure reported here was used as a search model and 4 copies were found in the asymmetric unit. A subsequent search with the variable and constant domains from the unliganded C05 Fab structure yielded good solutions for 4 complete Fab fragments. Rigid body refinement, simulated annealing and restrained refinement (including TLS refinement, with one group for HA1 and one for each Ig domain) were carried out in Phenix[47]. Riding hydrogens were used during refinement and are included in the final model. Between rounds of refinement, the model was built and adjusted using Coot[48]. Refinement statistics can be found in Supplementary Table 1.

Crystallization and structure determination of the C05-HK68/H3 HA trimer complex

Gel filtration fractions containing the C05-HK68/H3 trimeric HA complex were concentrated to ~10mg/mL in 10mM Tris, pH 8.0 and 50mM NaCl. Initial crystallization trials were set up using the automated Rigaku Crystalmation robotic system at the Joint Center for Structural Genomics (www.jcsg.org). Only two hits were obtained (in related conditions) and neither could be reproduced or optimized further. Thus, the crystals from the

initial screen were used for data collection. The best crystal was grown by the sitting drop vapor diffusion method with a reservoir solution (200 μL) containing 28% (w/v) PEG 400, 200mM calcium chloride, 100mM HEPES pH 7.5. Drops consisting of 100 nL protein + 100 nL precipitant were set up at 4°C, and a very small crystal was visible after 14 days. Over the course of a further 2 weeks, the crystal reached it maximum size. The crystal was cryoprotected by brief immersion in well solution supplemented with 10% ethylene glycol, then flash cooled and stored in liquid nitrogen until data collection.

Diffraction data for the C05-HK68/H3 trimer complex were collected on the GM/CA-CAT 23ID-B beamline at the Advanced Photo Source at Argonne National Laboratory. Due to poor crystal quality (cluster of stacked plates), the diffraction images were messy and highly anisotropic. The data were indexed in spacegroup P1, integrated and scaled using HKL2000 (HKL Research), and merged using Xprep (Bruker). The structure was solved by molecular replacement to a nominal resolution of 4.25 Å using Phaser[46]. However, due to the anisotropy of the diffraction, many reflections were observed at significantly higher resolution (~3.2 Å) than the nominal resolution reported, and these additional data were included in refinement. A HK68/H3 trimer from the high-resolution structure reported here was used as the initial search model and total of 4 trimers (12 HA protomers) were found in the asymmetric unit. The C05-HK68/H3 HA1 complex was docked onto each of the 12 HA1 subunits in the asymmetric unit to position the C05 Fab. Rigid body refinement, simulated annealing and restrained refinement (including TLS refinement, with one group for HA1, one for HA2, and one for each Ig domain) were carried out in Phenix[47]. Riding hydrogens were used during refinement and are included in the final model. Between rounds of refinement, the model was built and adjusted using Coot[48]. Refinement statistics can be found in Supplementary Table 1.

Structural analyses

Hydrogen bonds and van der Waals' contacts between C05 and the HK68/H3 HAl domain HA were calculated using HBPLUS and CONTACSYM, respectively. Surface area buried upon Fab binding was calculated with MS. MacPyMol (DeLano Scientific) and UCSF Chimera[49] was used to render structure figures and for general manipulations. Kabat numbering was applied to the coordinates using the AbNum server[37]. The final coordinates were validated using the JCSG quality control server (v2.7), which includes Molprobity[50]:

Sequence analysis of COS epitope conservation in all HA proteins

All full-length, non-redundant, and non-lab strain influenza A HA sequences were downloaded from the NCBI FLU database[34]. At the time of download (August 7, 2010), the dataset included 8720 sequences encompassing all 16 influenza A subtypes, of which 5813 and 2907 sequences were from group 1 and group 2 viruses, respectively. The sequences were aligned using MUSCLE[38] and analyzed using GCG (Accelrys) and custom shell scripts (available from the authors upon request). In this analysis, residues are considered conserved if substitutions are restricted to other amino acids in the same group: 1) Asp, Asn, Glu, GIn (negatively charged or isosteric polar substitutions); 2) Val, Ile, Leu, Met (small hydrophobic); 3) Phe and Tyr (aromatic); and 4) Ser and Thr (small polar/hydroxyl). The values reported for percent conservation are the number to sequences with an identical or conservative change at a position divided by the total number of sequences and multiplied by 100.

Supplementary Material

Refer to Web version on PubMed Central for supplementary material.

Acknowledgments

We thank H. Tien and D. Marciano of the Robotics Core at the JCSG for automated crystal screening, the staff of the APS GM/CA-CAT and SSRL BLII-I for beamline support, X. Dai and R Stanfield for assistance with data collection/processing M. Hothorn for assistance with ITC experiments, J. Paulson, and D. Burton for valuable comments and discussion, A. Estelles and R. Briante, L. Xu, S. Wang and D. Com for technical support, and P. Foreman for assistance with animal study design. This project was funded in part by NIH grant POI AI058 I 13 (LA.W.), a predoc-toral fellowship from the Achievement Rewards for College Scientists Foundation (D.C.E.), grant GM080209 from the NIH Molecular Evolution Training Program (D.C.E.), the Skaggs Institute (LA.W.), a career development fellowship from the Northeast Biodefense Center U54-AI057158-Lipkin (J.S.), NIAID grant U01AI070373 (R.W.), and CRIP, NIAID contract HHSN266200700010C (P.P.). Portions of this research were carried out at the Stanford Synchrotron Radiation Lightsource, a national user facility operated by Stanford University on behalf of the U.S. Department of Energy (DOE), Office of Basic Energy Sciences. The Stanford Synchrotron Radiation Lightsource (SSRL) Structural Molecular Biology Program is supported by the DOE Office of Biological and Environmental Research and by NIH, National Center for Research Resources, Biomedical Technology Program, and the National Institute of General Medical Sciences. The GM/CA CAT 23-ID-B beamline has been funded in whole or in part with federal funds from National Cancer Institute (Y1-CO-1020) and NIGMS (Y1-GM-1104). Use of the Advanced Photon Source (APS) was supported by the U.S. Department of Energy, Basic Energy Sciences, Office of Science, under contract no. DE-AC02-06CH11357. The electron microscopy data presented here was collected at the National Resource for Automated Molecular Microscopy which is supported by the National Institutes of Health though the National Center for Research Resources' P41 program (RR017573). The content is solely the responsibility of the authors and does not necessarily represent the official views of NIGMS or the NIH. This is publication 21421 from The Scripps Research Institute.

References

1. Smith TJ, Chase ES, Schmidt TJ, Olson NH, Baker TS. Neutralizing antibody to human rhinovirus 14 penetrates the receptor-binding canyon. Nature. 1996; 383:350–354. [PubMed: 8848050]
2. Labrijn AF, et al. Access of antibody molecules to the conserved coreceptor binding site on glycoprotein gp120 is sterically restricted on primary human immunodeficiency virus type 1. J Virol. 2003; 77:10557–10565. [PubMed: 12970440]
3. Rühlmann A, Kukla D, Schwager P, Bartels K, Huber R. Structure of the complex formed by bovine trypsin and bovine pancreatic trypsin inhibitor. Crystal structure determination and stereochemistry of the contact region. J Mol Biol. 1973; 77:417–436. [PubMed: 4737866]
4. McLellan JS, et al. Structure of HIV-1 gp120 V1/V2 domain with broadly neutralizing antibody PG9. Nature. 2011; 480:336–343. [PubMed: 22113616]
5. Pejchal R, et al. A potent and broad neutralizing antibody recognizes and penetrates the HIV glycan shield. Science. 2011; 334:1097–1103. [PubMed: 21998254]
6. Pejchal R, et al. Structure and function of broadly reactive antibody PG16 reveal an H3 subdomain that mediates potent neutralization of HIV-1. Proc Natl Acad Sci USA. 2010; 107:11483–11488. [PubMed: 20534513]
7. Kashyap AK, et al. Combinatorial antibody libraries from survivors of the Turkish H5N1 avian influenza outbreak reveal virus neutralization strategies. Proc Natl Acad Sci US A. 2008; 105:5986–5991.
8. Kashyap AK, et al. Protection from the 2009 H1N1 pandemic influenza by an antibody from combinatorial survivor-based libraries. PLoS Pathog. 2010; 6:e1000990. [PubMed: 20628565]
9. Ekiert DC, et al. Antibody recognition of a highly conserved influenza virus epitope. Science. 2009; 324:246–251. [PubMed: 19251591]
10. Throsby M, et al. Heterosubtypic neutralizing monoclonal antibodies cross-protective against H5N1 and H1N1 recovered from human IgM+ memory B cells. PLoS One. 2008; 3:e3942. [PubMed: 19079604]
11. Sui J, et al. Structural and functional bases for broad-spectrum neutralization of avian and human influenza A viruses. Nat Struct Mol Biol. 2009; 16:265–273. [PubMed: 19234466]
12. Ekiert DC, et al. A highly conserved neutralizing epitope on group 2 influenza A viruses. Science. 2011; 333:843–850. [PubMed: 21737702]
13. Corti D, et al. A neutralizing antibody selected from plasma cells that binds to group 1 and group 2 influenza A hemagglutinins. Science. 2011; 333:850–856. [PubMed: 21798894]

14. Corti D, et al. Heterosubtypic neutralizing antibodies are produced by individuals immunized with a seasonal influenza vaccine. J Clin Invest. 2010; 120:1663–1673. [PubMed: 20389023]
15. Wrammert J, et al. Broadly cross-reactive antibodies dominate the human B cell response against 2009 pandemic H1N1 influenza virus infection. J Exp Med. 2011; 208:181–193. [PubMed: 21220454]
16. Wei CJ, et al. Induction of broadly neutralizing H1N1 influenza antibodies by vaccination. Science. 2010; 329:1060–1064. [PubMed: 20647428]
17. Barbey-Martin C, et al. An antibody that prevents the hemagglutinin low pH fusogenic transition. Virology. 2002; 294:70–74. [PubMed: 11886266]
18. Fleury D, Wharton SA, Skehel JJ, Knossow M, Bizebard T. Antigen distortion allows influenza virus to escape neutralization. Nat Struct Biol. 1998; 5:119–123. [PubMed: 9461077]
19. Xu R, et al. Structural basis of preexisting immunity to the 2009 H1N1 pandemic influenza virus. Science. 2010; 328:357–360. [PubMed: 20339031]
20. Whittle JRR, et al. Broadly neutralizing human antibody that recognizes the receptor-binding pocket of influenza virus hemagglutinin. Proc Natl Acad Sci USA. 2011; 108:14216–14221. [PubMed: 21825125]
21. Fleury D, et al. A complex of influenza hemagglutinin with a neutralizing antibody that binds outside the virus receptor binding site. Nat Struct Biol. 1999; 6:530–534. [PubMed: 10360354]
22. Fleury D, Daniels RS, Skehel JJ, Knossow M, Bizebard T. Structural evidence for recognition of a single epitope by two distinct antibodies. Proteins. 2000; 40:572–578. [PubMed: 10899782]
23. Yoshida R, et al. Cross-protective potential of a novel monoclonal antibody directed against antigenic site B of the hemagglutinin of influenza A viruses. PLoS Pathog. 2009; 5:e1000350. [PubMed: 19300497]
24. Ohshima N, et al. Naturally occurring antibodies in humans can neutralize a variety of influenza virus strains, including H3, H1, H2, and H5. J Virol. 2011; 85:11048–11057. [PubMed: 21865387]
25. Okuno Y, Isegawa Y, Sasao F, Ueda S. A common neutralizing epitope conserved between the hemagglutinins of influenza A virus H1 and H2 strains. J Virol. 1993; 67:2552–2558. [PubMed: 7682624]
26. Lee H, et al. Reactivity-based one-pot synthesis of oligomannoses: defining antigens recognized by 2G12, a broadly neutralizing anti–HIV–1 antibody. Ang Chem Int Ed. 2004; 43:1000–1003.
27. Calarese DA, et al. Antibody domain exchange is an immunological solution to carbohydrate cluster recognition. Science. 2003; 300:2065–2071. [PubMed: 12829775]
28. Mouquet H, et al. Polyreactivity increases the apparent affinity of anti-HIV antibodies by heteroligation. Nature. 2010; 467:591–595. [PubMed: 20882016]
29. Pancera M, et al. Crystal structure of PG16 and chimeric dissection with somatically related PG9: structure-function analysis of two quaternary-specific antibodies that effectively neutralize HIV-1. J Virol. 2010; 84:8098–8110. [PubMed: 20538861]
30. Wilson PC, et al. Somatic hypermutation introduces insertions and deletions into immunoglobulin V genes. J Exp Med. 1998; 187:59–70. [PubMed: 9419211]
31. de Wildt RM, van Venrooij WJ, Winter G, Hoet RM, Tomlinson IM. Somatic insertions and deletions shape the human antibody repertoire. J Mol Biol. 1999; 294:701–710. [PubMed: 10610790]
32. Krause JC, et al. An insertion mutation that distorts antibody binding site architecture enhances function of a human antibody. mBio. 2011; 2:e00345–10. [PubMed: 21304166]
33. Zhou T, et al. Structural basis for broad and potent neutralization of HIV-1 by antibody VRC01. Science. 2010; 329:811–817. [PubMed: 20616231]
34. Bao Y, et al. The influenza virus resource at the National Center for Biotechnology Information. J Virol. 2008; 82:596–601. [PubMed: 17942553]
35. Hensley SE, et al. Hemagglutinin receptor binding avidity drives influenza A virus antigenic drift. Science. 2009; 326:734–736. [PubMed: 19900932]
36. Fleishman SJ, et al. Computational design of proteins targeting the conserved stem region of influenza hemagglutinin. Science. 2011; 332:816–821. [PubMed: 21566186]

37. Abhinandan KR, Martin AC. Analysis and improvements to Kabat and structurally correct numbering of antibody variable domains. Mol Immunol. 2008; 45:3832–3839. [PubMed: 18614234]
38. Edgar RC. MUSCLE: multiple sequence alignment with high accuracy and high throughput. Nucleic Acids Res. 2004; 32:1792–1797. [PubMed: 15034147]
39. Fodor E, et al. Rescue of influenza A virus from recombinant DNA. J Virol. 1999; 73:9679–9682. [PubMed: 10516084]
40. Miyazaki J, et al. Expression vector system based on the chicken beta-actin promoter directs efficient production of interleukin-5. Gene. 1989; 79:269–277. [PubMed: 2551778]
41. Brown PH, Cronan JE, Grotli M, Beckett D. The biotin repressor: modulation of allostery by corepressor analogs. J Mol Biol. 2004; 337:857–869. [PubMed: 15033356]
42. Lander GC, et al. Appion: an integrated, database-driven pipeline to facilitate EM image processing. J Struct Biol. 2009; 166:95–102. [PubMed: 19263523]
43. Voss NR, Yoshioka CK, Radermacher M, Potter CS, Carragher B. DoG Picker and TiltPicker: software tools to facilitate particle selection in single particle electron microscopy. J Struct Biol. 2009; 166:205–213. [PubMed: 19374019]
44. Mindell JA, Grigorieff N. Accurate determination of local defocus and specimen tilt in electron microscopy. J Struct Biol. 2003; 142:334–347. [PubMed: 12781660]
45. Hohn M, et al. SPARX, a new environment for Cryo-EM image processing. J Struct Biol. 2007; 157:47–55. [PubMed: 16931051]
46. McCoy AJ, et al. Phaser crystallographic software. J Appl Crystallogr. 2007; 40:658–674. [PubMed: 19461840]
47. Adams PD, et al. PHENIX: a comprehensive Python-based system for macromolecular structure solution. Acta Crystallogr D Biol Crystallogr. 2010; 66:213–221. [PubMed: 20124702]
48. Emsley P, Lohkamp B, Scott WG, Cowtan K. Features and development of Coot. Acta Crystallogr D Biol Crystallogr. 2010; 66:486–501. [PubMed: 20383002]
49. Pettersen EF, et al. UCSF Chimera--a visualization system for exploratory research and analysis. J Comput Chem. 2004; 25:1605–1612. [PubMed: 15264254]
50. Chen VB, et al. MolProbity: all-atom structure validation for macromolecular crystallography. Acta Crystallogr D Biol Crystallogr. 2010; 66:12–21. [PubMed: 20057044]

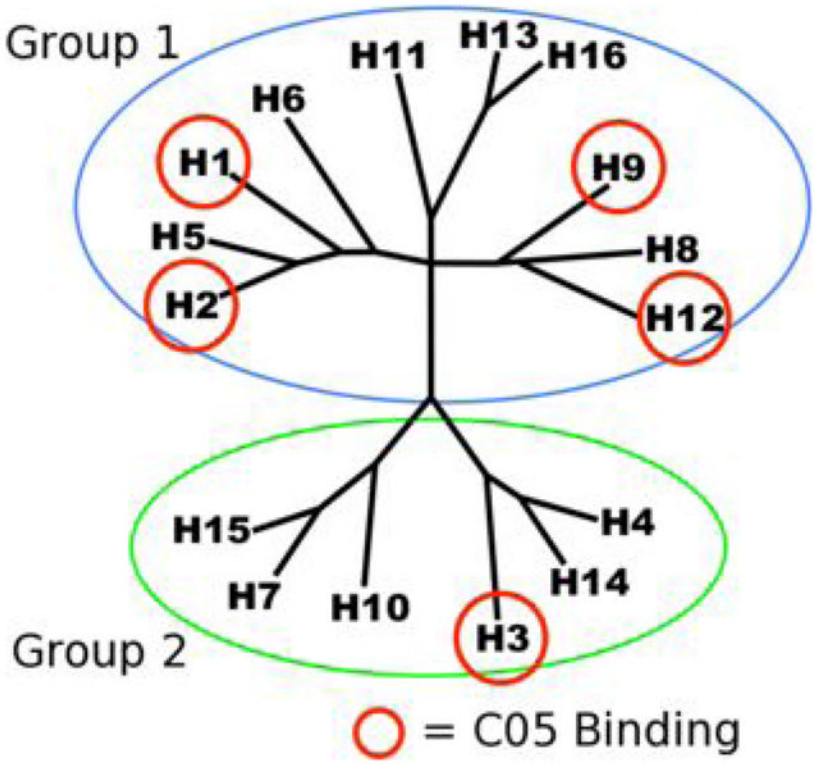

Figure 1. C05 neutralizes multiple influenza virus subtypes from groups 1 and 2

Phylogenetic tree with the two main viral lineages indicated with group 1 in the upper blue circle and group 2 in the lower green circle. Strains from subtypes circled in red are bound or neutralized by C05.

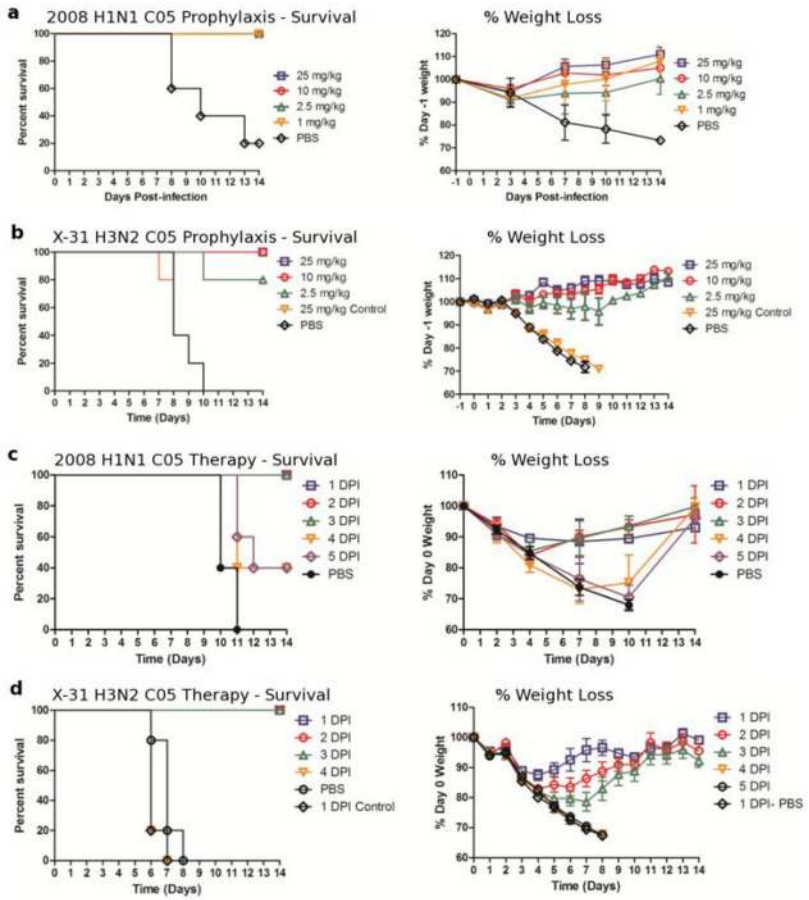

Figure 2. C05 protects mice from lethal virus challenge

Survival and weight loss were monitored in response to varying amounts of C05 IgG administered prophylactically to mice 24 hours before challenge with (**a**) 25x the 50% mouse lethal dose (MLD_{50}) of A/Memphis/3/2008 (H1N1) or (b) 33 MLD_{50} of A/Aichi/2/X-31/1968 (H3N2) viruses. A single therapeutic dose of 15 mg/kg C05 IgG was delivered 1, 2, 3, 4, or 5 days post-challenge with (**c**) 25 MLD_{50} of A/Memphis/3/2008 (H1N1) or (**d**) 33 MLD_{50} of A/Aichi/2/X-31/1968 (H3N2) viruses.

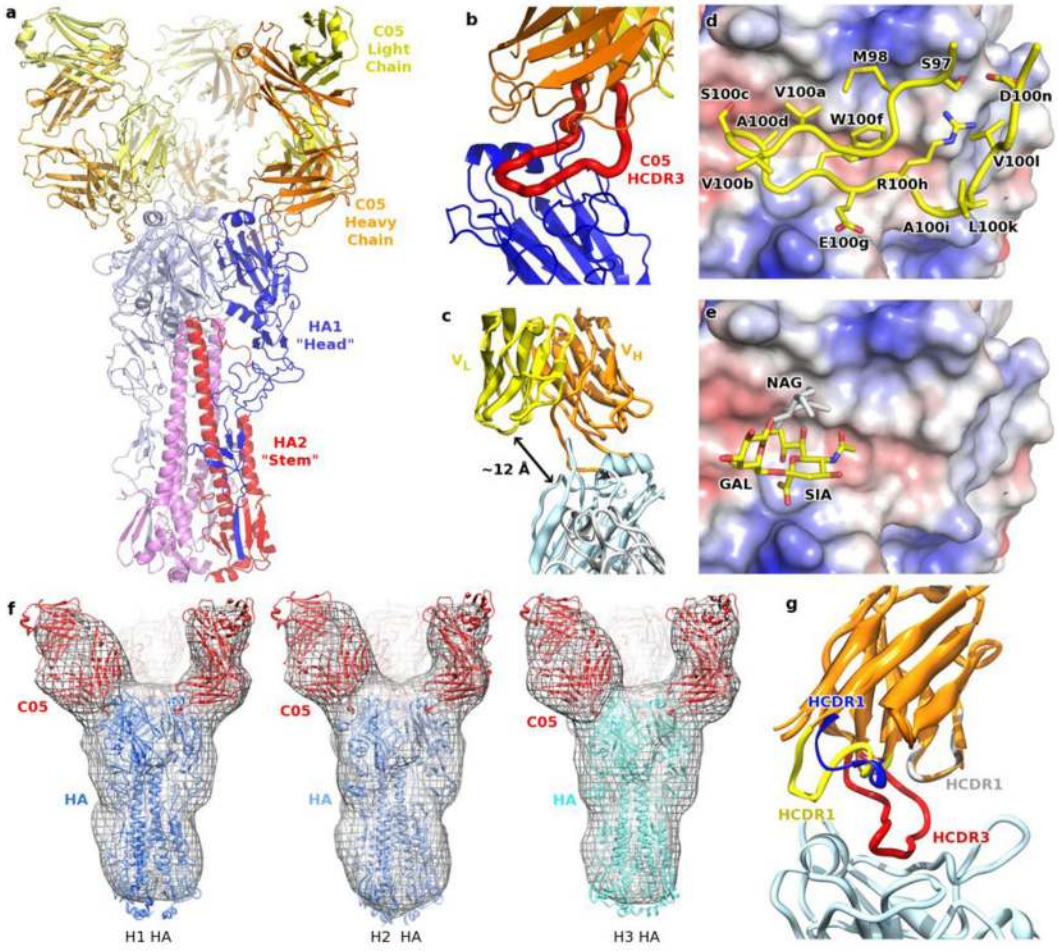

Figure 3. C05 binds the receptor binding site on the HA1 head

a, Crystal structures of C05 Fab in complex with trimeric HA and an HA1 fragment reveal the location of the C05 epitope in the HA1 "head" region. The C05 Fab heavy (orange) and light (yellow) chains and the HA1 (blue) and HA2 (red) subunits are depicted as ribbons. **b,** C05 inserts its long HCDR3 (red) into the receptor binding site. **c,** C05 binds HA using only its heavy chain. **d,** Interaction of the HA receptor binding pocket (in a solid electrostatic surface representation) with HCDR3 from C05 (in yellow backbone with side chains labeled by residue type and number) and **e,** with an α2,6 sialoglycan receptor (derived from PDB entry 1MQN), with an additional carbohydrate residue modeled in gray. The binding site for the C05 H3 loop and the glycan receptor overlap extensively. **f,** 3D EM reconstructions of C05 Fab (red) bound to H1 (blue), H2 (light blue), and H3 (cyan) HAs. Fitting of H1, H2, and H3 crystal structures into the reconstructions support a common binding mode of C05 to each of the HAs studied. **g,** In addition to its long HCDR3 (red), C05 has a 5-residue insertion in HCDR1 (yellow), extending the tip of this loop relative to the germline-encoded canonical conformation. For comparison, a sequence-related Fab structure (PDB code 2VXS) without an insertion in HCDR1 (blue loop) is superimposed on C05.

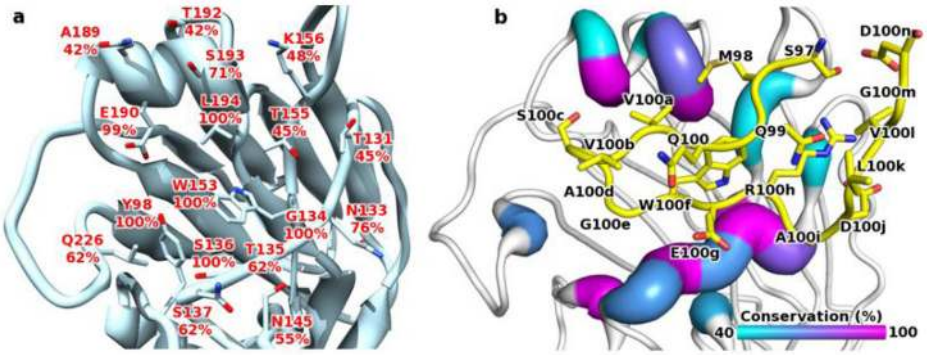

Figure 4. C05 epitope conservation across influenza A viruses

a, Due to the functional constraints imposed on the receptor binding site by interaction with sialyoglycans, many of residues that make up the C05 epitope are conserved among human influenza viruses. C05 contact residues are depicted as sticks and the percent conservation of each position across human H1, H2, and H3 viruses, the subtypes that have caused pandemics and epidemics in humans, is shown. **b,** Similar to the view in (**a**), but includes the position of C05's HCDR3 (yellow ribbon and sticks) relative to the epitope variation that is color coded on the HA backbone (with warmer colors indicating higher conservation). Contact residues on HA are depicted with a thick tube for their backbone, while non-contacting regions of HA are shown as a thin white ribbon.

Table 1

C05 binds and neutralizes multiple group 1 and group 2 influenza A viruses

a C05 neutralizes group 1 and group 2 influenza viruses in vitro

Grp	Subtype	Strain	MIC (μg/mL)
1	H1N1	A/Virginia/670/1987	>100[a]
		A/Texas/36/1991	>100[a]
		A/New Caledonia/20/1999	<0.1[a]
		A/Solomon Islands/2006	1.56[a]
		A/Brisbane/59/2007	1.56[a]
		A/Memphis/3/2008	<2.3[a]
		A/California/04/2009	>100[a]
	H2N2	A/Guiyang/1/1957	18[b]
	H5N1	A/Vietnam/1203/2004	>100[a]
	H9N2	A/Hong Kong/1073/1999	90[b]
2	H3N2	A/Aichi/2/X-31/1968	<0.1[a]
		A/Panama/2007/1999	0.39[a]
		A/Wisconsin/67/2005	<0.1[a]
		A/Brisbane/10/2007	12.5[a]

b C05 binding to group 1 and group 2 influenza hemagglutinins

Grp	Subtype	Strain	C05	CR6261	CR8020
1	H1N1	A/South Carolina/1/1918	–	++++	–
1	H1N1	A/New York/1/1918	–	++++	–
1	H1N1	A/AA/Marton/1943	–	++++	–
1	H1N1	A/USSR/90/1977	–	++++	–
1	H1N1	A/Singapore/6/1986	+	++++	–
1	H1N1	A/Texas/36/1991	–	++++	–
1	H1N1	A/Beijing/262/1995	+++	++++	–
1	H1N1	A/Solomon Islands/3/2006	+++	++++	–
1	H2N2	A/Japan/305/1957	+++	++	–
1	H2N2	A/Adachi/2/1957	+++	++	–
1	H5N1	A/Vietnam/1203/2004	–	++++	–
1	H5N1	A/Indonesia/05/2005	–	++++	–
1	H6N2	A/turkey/Massachusetts/3740/1965	–	++++	–
1	H9N2	A/turkey/Wisconsin/1/1966	+++	++++	–
1	H12N5	A/duck/Alberta/60/1976	+	–	–
1	H13N6	A/gull/Maryland/704/1977	–	++++	–
1	H16N3	A/black-headed gull/Sweden/4/99	–	+++	–
2	H3N2	A/duck/Ukraine/1/1963	–	–	++++

b C05 binding to group 1 and group 2 influenza hemagglutinins

Grp	Subtype	Strain	C05	CR6261	CR8020
2	H3N2	A/Hong Kong/1/1968	++	–	++++
2	H3N2	A/Bangkok/1/1979	–	–	++++
2	H3N2	A/Victoria/3/1975	–	–	++++
2	H3N2	A/Beijing/353/1989	–	–	++++
2	H3N2	A/Shangdong/9/1993	–	–	++++
2	H3N2	A/Panama/2007/1999	++	–	++++
2	H3N2	A/Moscow/10/1999	++	–	++++
2	H3N2	A/Brisbane/10/2007	+	–	++++
2	H3N2	A/Perth/16/2009	++++	–	++++
2	H4N6	A/duck/Czechoslovakia/1956	–	–	++
2	H7N7	A/Netherlands/219/2003	–	–	++++
2	H10N7	A/chicken/Germany/N/1949	–	–	++++
2	H14N5	A/mallard/Astrakhan/263/1982	–	–	++
2	H15N8	A/shearw./W.Australia/2576/1979	–	–	+++

C C05 exhibits unusually low affinity for some HAs from neutralized viruses

Grp	Subtype	Strain	C05 K_d (nM)		MIC (μg/mL)
			BLI	ITC	
2	H3N2	A/Perth/16/2009	18	26	n.d.
		A/Hong Kong/1/1968	430	100	<0.1
		A/Panama/2007/1999	720	225	0.4
		A/Brisbane/10/2007	>5000	~10,000	12.5

[a] hemagglutination inhibition (HAI)

[b] microneutralization (MN)

+, K_d ≥5000 nM

++, K_d = 500–5000 nM

+++, K_d = 50–500 nM

++++, K_d ≤50 nM

n.d., not determined

Table 2

Effect of HCDR1 mutations on C05 binding

	Dissociation Constants (K_d, nM)							
	C05 Variant							
Strain	**WT**	**del(FGEST)**	**Phe27b-A**	**Gly27c-Ala**	**Glu27d-Ala**	**Tyr31Phe**	**Tyr31Leu**	**Tyr31Ala**
A/Hong Kong/1/1968 (H3N2)	500	690	610	450	540	420	1400	640
A/Perth/13/2009 (H3N2)	18	1300	460	33	28	6.8	560	550

WT, wild type; del(FGEST), 5 residue deletion of HCDR1 residues 27b-28 predicted to prevent all interactions between HCDR1 and HA.